Shear Stress Measurements of a Vertically Impinging Planar Jet

Sara Hines, Lucas Vos

Background and Motivation

The project is to experimentally validate the findings of a numerical simulation for wall shear stress generated by a vertically impinging planar jet. Successful validation would allow the use of the in-house simulation software to further pursue a fundamental understanding of the physics of a wall jet generated by a vertically impinging planar jet.

Experiment Design and Setup

The general method of this experiment consists of calculating wall shear stress from velocity measurements obtained by a hot-wire anemometry system. The test apparatus consists of:

- Hot Wire Anemometer (Probe) (A)
- Planar jet nozzle and stand (B)
- Calibration tube with mass flow meter (C)
- 3-axis stepper-motor controlled arm (not shown)

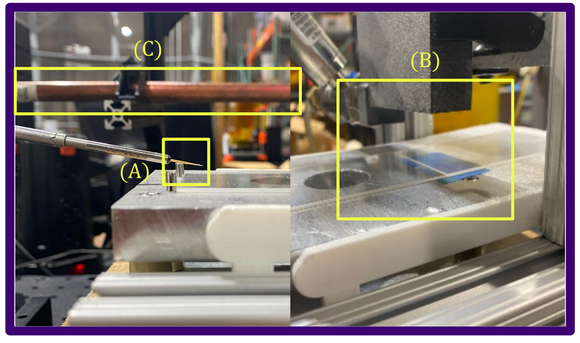

Fig 1: Test apparatus components

Calibration

The hot wire anemometer probe is a resistor in a wheatstone bridge in a feedback circuit that maintains the probe at a constant temperature. In operation, resistance of the probe decreases due to convective cooling and voltage across the horizontal of the bridge increases. The voltage across the horizontal feeds a servo amplifier to apply a proportional voltage across the vertical of the bridge, causing a current through the probe, heating the probe and increasing its resistance.

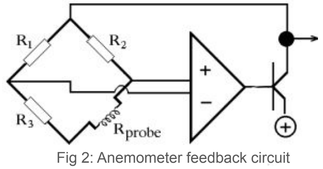

Fig 2: Anemometer feedback circuit

Since the anemometer maintains the probe at constant temperature, it is sensitive to the rate of cooling; the flow velocity. The hot wire probe is positioned at the center of a tube where maximum velocity of a turbulent flow will occur. Voltage measured by the anemometer is calibrated to velocity by mapping voltages to values of maximum velocity, where maximum velocities are determined from mass flow, air density, and cross sectional area of the tube.

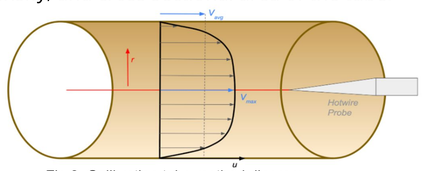

Fig 3: Calibration tube method diagram

Average velocity is calculated from maximum velocity using theoretical (**Eq.1**) and empirical (**Eq.2**) methods and plotted as a calibration curve, shown in **Fig. 4**.

(1) $u_{avg} = u_{max}\left(\frac{2\beta\left(\frac{2}{m}, \frac{n+1}{n}\right)}{m}\right)$ **(2)** $u_{max} = u_{avg}(1 + 1.33(Fr)^{1/2})$

Where β is the beta function with determined inputs m and n, and the friction factor, Fr, is a function of Reynolds number.

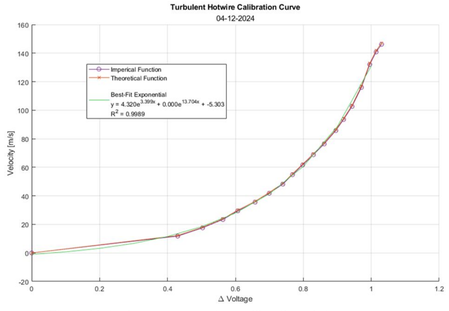

Fig 4: Hot wire anemometer calibration data

Data Collection

The hot wire probe attached to the 3-axis arm can move in increments as small as 0.1mm. The probe is oriented perpendicular to the planar jet and positioned at the surface of a glass pane underneath the planar jet. Motion of the probe is automated, pausing at each point while voltage is recorded before moving to the next point.

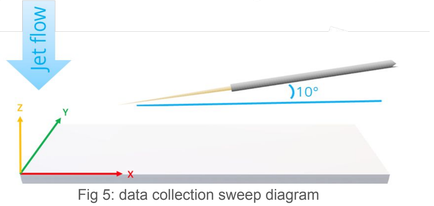

Fig 5: data collection sweep diagram

Data Analysis

After the voltage profile is collected, it is then compared against the calibration curve to establish the velocity profile across the plate. This profile is shown in **Fig. 6**.

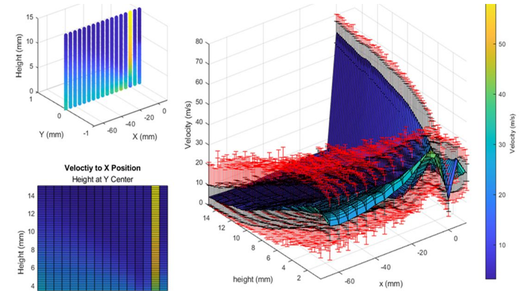

Fig 6: 3D velocity profile at center Y plane

The horizontal flow velocity near a wall is tied to the height of a reference point above the laminar sublayer, known as the boundary layer. **Fig. 7** below helps visualize this relationship for select discrete x values.

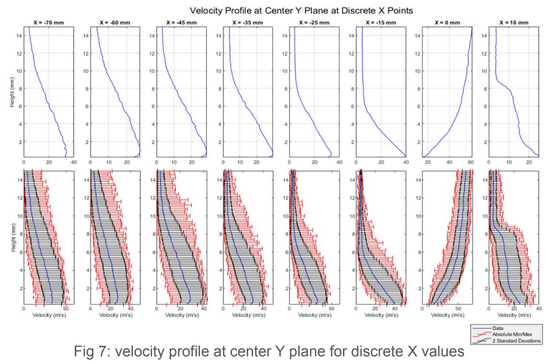

Fig 7: velocity profile at center Y plane for discrete X values

The logarithmic law of the wall (**Eq.3**) computes the wall shear stress using the linear relationship in the log-law region. With standard sea-level values for kinematic viscosity, fluid density, and constants (Von Karman constant K and C+), the friction velocity (**Eq.4**) and wall shear stress can be determined from collected velocity (**Eq.5**) and height data (**Eq.6**).

(3) $u^+ = \frac{1}{\kappa} \ln y^+ + C^+$ **(4)** $u_\tau = \sqrt{\frac{\tau_w}{\rho}}$

(5) $u^+ = \frac{u}{u_\tau}$ **(6)** $y^+ = \frac{y\, u_\tau}{\nu}$

In near-wall flow, sublayers and natural flow phenomena necessitate isolating the linear velocity region where the law of the wall applies. Wall shear stress for each (x, y) point is then averaged from the calculated shear at each respective height. This profile is plotted below in **Fig. 8** and the distribution is visualized in **Fig. 9**.

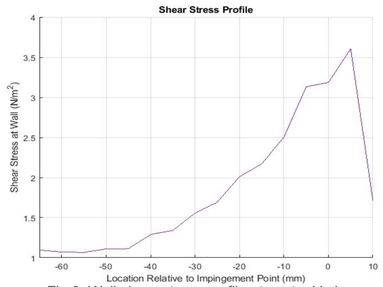

Fig 8: Wall shear stress profile at center Y plane

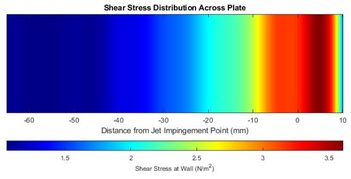

Fig 9: Wall shear stress distribution

The shear stress peaks just after the impingement point and drops asymptomatically across the length of the plate. The general shape of the wall shear stress profile follows the trends expected by simulations, but the magnitudes of shear stress fall below projections based on nozzle pressure ratio.

Future Work

Next steps for this project include review of the analytical code and assumptions made to diagnose the discrepancy between projected and calculated shear stress. With discrepancies resolved, more data points along the center Y plane will be taken to smooth profile plots for sharper analysis and sweeps in consecutive Y planes will allow for shear stress distributions along the entire wall surface.

Acknowledgements: We thank our advisor, Professor Dana Dabiri for his guidance on this project, Professor Igor Novosselov for use of his facility space and equipment, Benito Chacko for his significant contribution to the analytical code and development of the project, Richard Egbert and Ben Fetters for the design and manufacturing of the nozzle and test stand, and Anthony Tang for his technical assistance.